

---

# Supplement to: Learning abstract structure for drawing by efficient motor program induction

---

Anonymous Author(s)

Affiliation

Address

email

## 1 Program synthesis algorithm

The algorithmic engine behind our program synthesis method follows the approach introduced in EC<sup>2</sup> [1], and is based on the open source implementation of EC<sup>2</sup>'s successor, DreamCoder [2]. Our program induction model takes as input a corpus of black-and-white raster **training images**, and seeks to synthesize a graphics program that generates each of them. The model estimates a prior over programs for training images, to be deployed on held-out **test images**. Following [2] we now derive this algorithm starting from a Bayesian viewpoint. With this probabilistic formalism in hand we will then briefly outline the 3-step algorithm which performs inference in this model, but interested readers should consult [2, 1] for a complete algorithmic exposition.

**Notation.** We write  $I$  to mean an image, and  $\rho$  to mean a graphics program. Programs are represented in typed lambda calculus. Initially the graphics programming language contains the **primitives** outlined in Table 1 of the main text. Primitives are expressions in typed lambda calculus.

We write  $\llbracket \rho \rrbracket$  to mean the image output by program  $\rho$ . We write  $L$  to mean a **library** of primitives; At the initial state of learning  $L$  contains the primitives in Table 1 of the main text. The library  $L$  acts as a prior over the space of programs, written  $P(\cdot|L)$  and defined formally in [2]. Intuitively, this prior prefers programs which may be expressed compactly using the primitives in  $L$ . We write  $P(L)$  to mean the prior probability of the library  $L$ , and this prior prefers libraries which overall contain less code (smaller lambda calculus expressions).

From a Bayesian point of view our aim is to estimate the prior maximizing the joint probability, which we will notate  $J$ :

$$P(L|\{I_n\}_{n=1}^N) \propto P(L, \{I_n\}_{n=1}^N) = J(L) = P(L) \prod_{n=1}^N \sum_{\rho} P(I_n|\rho)P(\rho|L) \quad (1)$$

where  $P(I|\rho) = \mathbb{1}[I = \llbracket \rho \rrbracket]$ . Evaluating this objective is intractable because it requires marginalizing over the infinite set of all programs. We define the following intuitive lower bound, written  $\mathcal{L}$ , on this objective function:

$$J(L) \geq \mathcal{L}(L, \{\mathcal{B}_{I_n}\}_{n=1}^N) = P(L) \prod_{1 \leq n \leq N} \sum_{\rho \in \mathcal{B}_{I_n}} P(I_n|\rho)P(\rho|L) \quad (2)$$

where the bound  $\mathcal{L}$  is expressed in terms of a collection of sets of programs,  $\{\mathcal{B}_n\}_{n=1}^N$ , called **beams**:

**Definition.** A **beam** for image  $I$  is a finite set of programs where, for any  $\rho \in \mathcal{B}_I$ , we have  $P(I|\rho) > 0$ . In other words, every program in the beam for image  $I$  correctly draws  $I$ .

Making the beams finite ensures that calculation of  $\mathcal{L}$  is tractable. In our experiments we bounded the size of the beams to 5.

We alternate maximization of  $\mathcal{L}$  with respect to the beams and the library. In reference to figure 2 of the main text, these alternate maximization steps are called the **Explore** and **Compress** steps.

32 **Explore: Maxing  $\mathcal{L}$  w.r.t. the beams.** Here  $L$  is fixed and we want to find new programs to add to  
 33 the beams so that  $\mathcal{L}$  increases the most.  $\mathcal{L}$  most increases by finding programs where  $P[I|\rho]P[\rho|L]$   
 34 is largest.

35 **Compress: Maxing  $\mathcal{L}$  w.r.t. the library.** Here  $\{\mathcal{B}_{I_n}\}_{n=1}^N$  is held fixed, and so we can evaluate  $\mathcal{L}$ .  
 36 Now the problem is that of searching the discrete space of libraries and finding one maximizing  $\mathcal{L}$ .

37 Searching for programs is hard because of the large combinatorial search space. We ease this difficulty  
 38 by training a neural recognition model,  $Q(\cdot|\cdot)$ , during the Compile step:  $Q$  is trained to approximate  
 39 the posterior over programs,  $Q(\rho|I) \approx P(\rho|I, L)$ , thus amortizing the cost of finding programs with  
 40 high posterior probability.

41 **Compile: learning to tractably maximize  $\mathcal{L}$  w.r.t. the beams.** Here we train  $Q(\rho|I)$  to assign  
 42 high probability to programs  $\rho$  where  $P(x|p)P(p|L)$  is large, because including those programs in  
 43 the beams will most increase  $\mathcal{L}$ . We train  $Q$  both on programs found during the Explore step and on  
 44 samples from the current library, i.e.  $P(\cdot|L)$ . Assuming that  $Q$  successfully converges to the true  
 45 posterior estimates, then incorporating these top programs as measured by  $Q$  into the beams will  
 46 maximally increase  $\mathcal{L}$ .

## 47 1.1 Algorithmic details

48 Having introduced the probabilistic framing of our problem, and the 3-step inference procedure, we  
 49 now briefly outline the algorithmic implementation of the explore/compress/compile steps. A full  
 50 overview is contained in [2].

### 51 1.1.1 Explore

52 During the Explore step we enumerate programs in decreasing order under  $Q(\cdot|I_n)$  for each image  $I_n$ ,  
 53 and keep the top 5 within the beam  $\mathcal{B}_{I_n}$  as measured by the posterior  $P(\rho|I_n, L)$ . This enumeration  
 54 is tractable given our parameterization of  $Q$ , which can be expressed similarly to a PCFG over  
 55 programs; i.e., the neural network outputs a distribution over programs parameterized by the weights  
 56 of a probabilistic grammar, and we enumerate in decreasing order under that grammar. Thus,  $Q$   
 57 outputs the transition probabilities of a bigram model over program syntax trees, which may be  
 58 unrolled into a PCFG-like representation. Enumeration proceeds until a per-image timeout is reached;  
 59 we used a timeout of one hour.

### 60 1.1.2 Compress

61 Here we seek to update the library by increasing the probability it assigns to programs in the beams,  
 62 hence “compressing” those programs. Indeed the compress objective can be rewritten in terms of a  
 63 sum of description lengths:

$$\arg \max_L \mathcal{L} = \arg \min_L \underbrace{-\log P(L)}_{\text{description length of library}} + \sum_{1 \leq n \leq N} \underbrace{-\log \sum_{\rho \in \mathcal{B}_{I_n}} P(I_n|\rho)P(\rho|L)}_{\text{description length of program generating image } I_n} \quad (3)$$

64 To heuristically minimize this description length we search locally through the space of libraries  $L$   
 65 until the above objective fails to improve. Our search moves consist of incorporating new subex-  
 66 pressions obtained from automatically refactoring programs in the beams—intuitively, refactoring  
 67 programs that we found explaining images so as to minimize the total size of the library plus the  
 68 total size of those programs. This refactoring process combines version space algebra [3] with  
 69 equivalence graphs [4], which are two approaches from the programming languages and program  
 70 synthesis community; see [2] for details.

### 71 1.1.3 Compile

72 Here we train a neural network to guide the search over programs, seeking to minimize its divergence  
 73 from the true posteriors over programs. Writing  $\phi$  for the parameters of  $Q$ , we aim to maximize

$$\arg \max_{\phi} \mathbb{E} \left[ Q_{\phi} \left( \left( \arg \max_{\rho} P(\rho|L, I) \right) \mid I \right) \right] \quad (4)$$

74 where the expectation is taken over images  $I$ . Taking this expectation over the empirical distribution  
75 of images trains the network on programs found during the Explore step; taking the expectation over  
76 samples, or “dreams,” from the learned prior  $L$ . Training on dreams is critical for sample efficiency:  
77 just like humans our model learns from at most a few dozen images, which is too little training data  
78 for a high-capacity neural network. But as we learn our prior, we can then draw unlimited dreams to  
79 train the neural network.

## 80 1.2 Generalizing to test images

81 Prior to evaluation on test images we iterate this learning procedure for 20 cycles (of searching  
82 for task solutions, updating the library, and training the neural network). The end state of learning  
83 is not just a program for each training image but, critically, also a learned inductive bias  $L$  and a  
84 learned inference/synthesis strategy  $Q$ . When comparing with human data we infer a program for  
85 test images by enumerating programs in decreasing order under  $Q(\cdot|I)$  and then rescore under  
86  $P_{\text{test}}(I|\rho)P(\rho|L)$ , where the likelihood  $P_{\text{test}}(I|\rho) \propto \exp(-\|I - \llbracket \rho \rrbracket\|_2)$  is a relaxed version of the 0/1  
87 likelihood during train to allow partial credit when the model cannot fully explain a test image.

## 88 2 Analysis of behavior

### 89 2.1 Converting a motor trajectory into a sequence of discrete strokes

90 Motor trajectories [raw data in the form of coordinates and corresponding times  $(x, y, t)$ ] were  
91 segmented into discrete “strokes”. Each stroke was a sequence of coordinates during which the  
92 finger was continuously touching the screen; i.e., strokes were separated by no-touch gaps. Subjects  
93 naturally tended to lift their finger between each discrete segment (i.e., line or circle) in the drawing.

94 Each stroke was summarized in a stroke-level feature vector  $\phi_{\text{stroke}} = (\text{category}, \text{startLocation},$   
95  $\text{center}, \text{row}, \text{column})$ . *category* is the type of object represented by the stroke, either a “vertical line”  
96 (LL), “horizontal line” (Lh), or “circle” (C). *startLocation* is the  $(x, y)$  position of the stroke onset.  
97 *row* and *column* were defined by “snapping” a stroke onto its position in a  $3 \times N$  (row  $\times$  column)  
98 grid, where  $N$  is the number of vertical lines in the “grating” for a given stimulus.

99 An entire trajectory  $t$  was therefore defined by the ordered list of strokes:  $(\phi_{\text{stroke}}^1, \phi_{\text{stroke}}^2, \dots)$ .

100 To calculate frequencies of horizontal/vertical transitions in a given trajectory, stroke transitions were  
101 classified as either horizontal (same row, different column), vertical (same column), or undefined  
102 (different row, different column).

### 103 2.2 Motor Cost model: extracting motor cost features from motor trajectories

104 We define a *feature extractor*  $\phi(\cdot)$  that maps a trajectory  $t$  to a trajectory-level real-valued feature  
105 vector  $\phi(t)$  with four elements based *a priori* on known drawing biases [5, 6]: *start*, *distance*,  
106 *direction*, and one meant to capture biases reflecting learning in this task *verticality*.

107 *start* is position of first touch, represented as distance from the top-left corner. *distance* is the  
108 summed distance traveled, measured as the path between stroke centers, *direction* is the summed  
109 distance travelled, but projected onto the diagonal from top-left to bottom-right, a direction chosen  
110 because it is a common bias in sketching and writing. *verticality* is the cumulative distance moved  
111 projected onto the y-axis subtracting distance projected onto the x-axis, and was included to allow the  
112 Motor Cost models trained on separate groups (MC1 and MC2) to capture learned directional biases.

### 113 2.3 Extending motor cost features to quantify program-like structure in behavior

114 In order to quantify variation in behavior across subjects, we fit the Motor Cost model to each subject,  
115 but with the model extended with two parameters in addition to the four described above, *chunking*  
116 and *skewers*. *chunking* was the count of the number of transitions between strokes of identical  
117 categories (e.g., circle  $\rightarrow$  circle), which reflects a bias to group similar objects together. *skewers*  
118 quantifies whether transitions away from “long vertical line” tend to be vertical (reflecting a bias to  
119 draw skewers) or horizontal (reflecting a bias to draw gratings); this was implemented similarly to  
120 *verticality*.

Subjects exhibited program-like structure as described in Figure 4 in the main text. Assignment of subjects to different strategies was supported both by visual inspection of their behavior and of their features from fitting this extended Motor Cost model (Supplemental Figure 1). We found the outcomes of these two methods to be largely in agreement. We note that subjects did tend to form a continuum between these four strategies, and so we attempted to assign the dominant strategy.

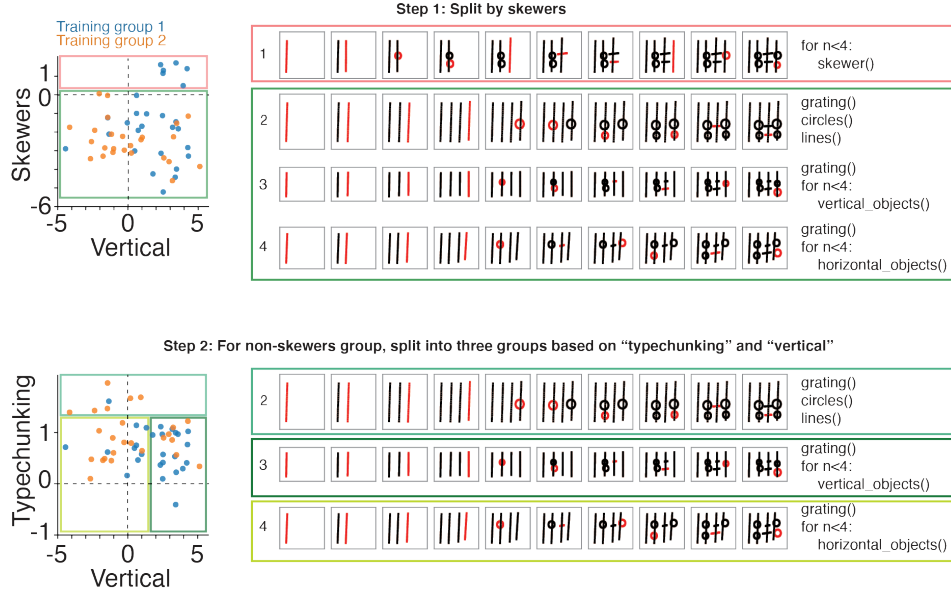


Figure 1: Quantitation of diversity of program-like strategies. Left scatter plots: datapoints represent values of Motor Cost model features for individual subjects along three dimensions: “skewers”, “vertical”, and “typechunking” are Motor Cost model features. Top row: first, subjects were grouped into those drawing “skewers” and those drawing “gratings” (Step 1). Bottom row: second, the “gratings” group was split into three groups based on what they drew immediately after drawing gratings (Step 2). These two steps led to four mutually exclusive groups. Colored boxes allow for comparison between the scatterplots (left) and example motor sequences (right).

### 3 Datasets

Included are behavioral data from all experiments in this paper.

**Supplementary\_dataset\_1.pickle** Data from 54 subjects in the main experiment.

**Supplementary\_dataset\_2.pickle** Data from 50 subjects in the followup experiment (rotated test stimuli).

### References

- [1] Kevin Ellis, Lucas Morales, Mathias Sablé-Meyer, Armando Solar-Lezama, and Josh Tenenbaum. Library learning for neurally-guided bayesian program induction. In *NeurIPS*, 2018.
- [2] Kevin Ellis, Catherine Wong, Maxwell Nye, Mathias Sablé-Meyer, Luc Cary, Lucas Morales, Luke Hewitt, Armando Solar-Lezama, and Joshua Tenenbaum. Dreamcoder: Growing generalizable, interpretable knowledge with wake-sleep bayesian program learning. *ArXiv preprint*, 2020.
- [3] Tessa Lau, Steven A Wolfman, Pedro Domingos, and Daniel S Weld. Programming by demonstration using version space algebra. *Machine Learning*, 53(1-2):111–156, 2003.
- [4] Ross Tate, Michael Stepp, Zachary Tatlock, and Sorin Lerner. Equality saturation: a new approach to optimization. In *ACM SIGPLAN Notices*, volume 44, pages 264–276. ACM, 2009.
- [5] Brenden M Lake, Ruslan Salakhutdinov, and Joshua B Tenenbaum. Human-level concept learning through probabilistic program induction. *Science*, 350(6266):1332–1338, 2015.

143 [6] Peter Van Sommers. *Drawing and cognition: Descriptive and experimental studies of graphic production*  
144 *processes*. Cambridge University Press, 1984.